EBioMedicine 7 (2016) 146–156

Contents lists available at ScienceDirect

EBioMedicine

journal homepage: www.ebiomedicine.com

Research Paper

Targeting the PDGF-B/PDGFR-β Interface with Destruxin A5 to Selectively Block PDGF-BB/PDGFR-ββ Signaling and Attenuate Liver Fibrosis

Xingqi Wang [a,b,1], Xuefeng Wu [a,1], Aihua Zhang [a,1], Shiyu Wang [a], Chunhui Hu [a], Wei Chen [a], Yan Shen [a], Renxiang Tan [a,*], Yang Sun [a,*], Qiang Xu [a,*]

[a] State Key Laboratory of Pharmaceutical Biotechnology, School of Life Sciences, Nanjing University, 22 Hankou Road, Nanjing 210093, China
[b] Key Laboratory for Biotechnology on Medicinal Plants of Jiangsu Province, School of Life Science, Jiangsu Normal University, Xuzhou 221116, China

ARTICLE INFO

Article history:
Received 24 November 2015
Received in revised form 12 March 2016
Accepted 29 March 2016
Available online 4 April 2016

Keywords:
Destruxin A5
PDGF-B/PDGFR-β
Protein–protein interface
Selective inhibitor
Liver fibrosis

ABSTRACT

PDGF-BB/PDGFR-ββ signaling plays very crucial roles in the process of many diseases such as liver fibrosis. However, drug candidates with selective affinities for PDGF-B/PDGFR-β remain deficient. Here, we identified a natural cyclopeptide termed destruxin A5 that effectively inhibits PDGF-BB-induced PDGFR-β signaling. Interestingly and importantly, the inhibitory mechanism is distinct from the mechanism of tyrosine kinase inhibitors because destruxin A5 does not have the ability to bind to the ATP-binding pocket of PDGFR-β. Using Biacore T200 technology, thermal shift technology, microscale thermophoresis technology and computational analysis, we confirmed that destruxin A5 selectively targets the PDGF-B/PDGFR-β interaction interface to block this signaling. Additionally, the inhibitory effect of destruxin A5 on PDGF-BB/PDGFR-ββ signaling was verified using *in vitro*, *ex vivo* and *in vivo* models, in which the extent of liver fibrosis was effectively alleviated by destruxin A5. In summary, destruxin A5 may represent an efficacious and more selective inhibitor of PDGF-BB/PDGFR-ββ signaling.

1. Introduction

Platelet-derived growth factor receptor-beta (PDGFR-β) is a cell surface receptor tyrosine kinase (Arora and Scholar, 2005). The biological effect of PDGFR-β is initiated through binding to its ligands PDGF-B or PDGF-D (Andrae et al., 2008; Borkham-Kamphorst et al., 2015; Kondo et al., 2013). Accumulating documents have revealed that PDGF-B, as the crucial ligand of PDGFR-β, binds to the extracellular domain of PDGFR-β to promote its dimerization, which initiates PDGF-BB/PDGFR-ββ signaling (Shim et al., 2010). The structure of the PDGF-B/PDGFR-β complex revealed that PDGFR-β is bound by two PDGF-B promoters, and the interface of the PDGF-B/PDGFR-β complex is predominantly hydrophobic (Shim et al., 2010).

Excessively enhanced PDGF-BB/PDGFR-ββ signaling is an important feature of liver fibrosis (Kocabayoglu et al., 2015). The underlying cellular mechanisms of liver fibrosis principally involve the activation of hepatic stellate cells (HSCs) which are the principal fibrogenic cell type in the liver (Bonner, 2004). Following chronic liver injury, HSCs differentiate from quiescent cells into proliferative myofibroblasts, which are an activated type of HSCs (Bataller and Brenner, 2005). During this transition, activated HSCs up-regulate the expression of PDGFR-β, whereas the level of PDGFR-β is low in healthy livers (Bonner, 2004; Kocabayoglu et al., 2015). Additionally, the paracrine signaling molecules released by other resident liver cells can also enhance the expressions of PDGF-B and PDGFR-β in activated HSCs (Bonner, 2004). However, the level of PDGFR-α expression by HSCs remains unchanged during liver injury (Bonner, 2004).

It is well known that PDGF-BB/PDGFR-ββ signaling is the most potent mitogenic pathway in HSC activation and fibrogenesis (Bonner, 2004; Kocabayoglu et al., 2015). Patients with liver cirrhosis caused by chronic hepatitis C exhibit more extensive platelet areas in the liver compared with normal livers, and HSCs expressing PDGFR-β are frequently observed in the areas with extensive platelets (Kondo et al., 2013). The PDGF-BB/PDGFR-ββ axis represents an appealing target for the treatment of liver fibrosis (Kocabayoglu et al., 2015; Prosser et al., 2006; Yoshida et al., 2014); specifically, antagonism of this axis has the potential to serve as an anti-fibrotic strategy. Previous studies have revealed that some receptor tyrosine kinase inhibitors, such as imatinib, sorafenib and sunitinib, whose targets include PDGFR-β, inhibit HSC activation and mitigate fibrosis (Majumder et al., 2013; Westra et al., 2014). However, these drugs are nonselective PDGFR-β inhibitors that were originally used to treat cancers in the clinic (Ehnman and

Abbreviations: ALT, alanine aminotransferase; AST, aspartate aminotransferase; BDL, bile duct ligation; EGFR, epidermal growth factor receptor; FBS, fetal bovine serum; FLT3, FMS-like tyrosine kinase 3; HBV, hepatitis B virus; HAS, human serum albumin; HSC, hepatic stellate cell; PDGF, platelet-derived growth factor; PDGFR, platelet-derived growth factor receptor; PI, propidium iodide; RU, relative units; SPR, surface plasmon resonance; VEGFR, vascular endothelial growth factor receptor.

* Corresponding authors.
E-mail addresses: rxtan@nju.edu.cn (R. Tan), yangsun@nju.edu.cn (Y. Sun), molpharm@163.com (Q. Xu).

[1] These authors contributed equally to this work.

http://dx.doi.org/10.1016/j.ebiom.2016.03.042

Östman, 2014), and their use may lead to unwanted side effects in patients affected only by the PDGFR-β-related diseases. In order to make anti-fibrotic drugs selectively target the activated HSCs, Brennand et al. constructed a cyclic peptide analog of PDGF-BB$^{73-81}$ (^{77}IVRKK^{81}-C-^{73}RKIE^{78}) that can prevent PDGF-BB from binding to its receptor and inhibit PDGF-BB-induced DNA synthesis in human fibroblasts (Brennand et al., 1997), whereas there are no data to support its *in vivo* effects. Beljaars et al. constructed a macromolecule with affinity for PDGFR-β by modification of human serum albumin (HSA) with a cyclic octapeptide (called pPB) that recognizes the PDGFR-β (Beljaars et al., 2003). This macromolecule (pPB-HSA) is able to reduce PDGF-BB-induced fibroblast proliferation *in vitro* (Beljaars et al., 2003). However, pPB alone has no ability to compete with the cellular binding of PDGF-BB within 0–125 μM (Beljaars et al., 2003). Notably, pPB-HAS and bicyclic pPB fail to exert anti-fibrotic effects on mice administered with CCl_4 (Bansal et al., 2011, 2014). Therefore, pPB and BipPB modified proteins are predominantly used as targeting devices to selectively interact with cells, predominantly (myo) fibroblasts, that express the PDGF-β receptor (Bansal et al., 2011, 2014; Beljaars et al., 2003). Therefore, more efficacious and selective drug candidates targeting the PDGF-BB/PDGFR-ββ axis are still lacking. These considerations impelled us to explore an alternative therapeutic approach to more selectively block the PDGF-BB/PDGFR-ββ axis. After screening of multiple compounds, we found that destruxin A5, a natural cyclopeptide which has insecticidal and anti-inflammatory effects (Krasnoff et al., 1996; Zhang et al., 2013), represents a therapeutic option for liver fibrosis. Herein, we describe a highly efficacious inhibitory approach involving destruxin A5 to selectively block PDGF-BB/PDGFR-ββ signaling by targeting PDGFR-β to occupy the protein–protein binding interface between PDGF-B and PDGFR-β.

2. Materials and Methods

2.1. Mice and Reagents

Destruxin A5 was isolated and identified as reported by us previously (Zhang et al., 2013). Detailed information on mice and reagents is provided in the Supplemental Experimental Procedures.

2.2. Cell Culture and Cell Proliferation Assay

The immortalized human HSC line LX-2 and activated rat HSC line CFSC-8B were maintained in new plastic culture dishes in Dulbecco's modified Eagle's medium supplemented with 100 μg/ml of streptomycin, 100 U/ml of penicillin and 10% fetal bovine serum (FBS) under a humidified 5% (v/v) CO_2 atmosphere at 37 °C. Cell proliferation was determined by MTT assay, as we have previously reported (Wang et al., 2014).

2.3. Surface Plasmon Resonance (SPR)

We performed SPR assays using the Biacore T200. Detailed information is provided in the Supplemental Experimental Procedures.

2.4. HSC Migration Assay

The migratory capacities of the cells were investigated as described previously (Liu et al., 2011). Detailed information is provided in the Supplemental Experimental Procedures.

2.5. HSC Wound Healing Assay

For the determination of cell migration during wound healing, a wound healing assay was performed as described previously (Rodriguez et al., 2005). Detailed information is provided in the Supplemental Experimental Procedures.

2.6. Western Blot

Proteins were extracted in lysis buffer. The proteins were then separated by SDS-PAGE (10%) and electrophoretically transferred onto polyvinylidene fluoride membranes. The membranes were probed with antibodies overnight at 4 °C, and then incubated with a HRP-coupled secondary antibody. Detection was performed using a LumiGLO chemiluminescent substrate system (KPL, Guildford, UK).

2.7. Cell Cycle Assay

This work was performed as we previously reported (Wang et al., 2015b). Detailed information is provided in the Supplemental Experimental Procedures.

2.8. Cell Apoptosis Assay

HSCs were seeded in 6-well plates in Dulbecco's modified Eagle's medium and treated with or without destruxin A5 for 24 h. Cell apoptosis was determined by flow cytometry after addition of FITC-conjugated annexin V and PI assay. Samples were analyzed by flow cytrometry on a FACScan (Becton Dickinson). Data were analyzed with CELLQuest software (BD Biosciences).

2.9. Immunohistochemistry

Paraffin-embedded liver sections were heat-fixed, blocked with 3% H_2O_2, and incubated with specific antibodies (1:100 diluted) overnight at 4–8 °C. Detection was done using Real Envision Detection kit from GeneTech Company (Shanghai, China) according to the manufacturer's instructions.

2.10. Real-time Quantitative PCR

This work was performed as we previously reported (Wang et al., 2015a). Detailed information is provided in the Supplemental Experimental Procedures.

2.11. Cultivation and Metabolites Isolation

Detailed information is provided in the Supplemental Experimental Procedures.

2.12. Models of Murine Liver Fibrosis

Liver fibrosis was induced by ligation of the common bile duct (BDL) (Liu et al., 2011). Mice (8–10 weeks, n = 8 in each group) were anesthetized. Following midline laparotomy, the common bile duct was double ligated and transected between the ligatures. The sham group was subjected to a similar operation without BDL. After BDL for 6 d, destruxin A5 was administered at 5–10 mg/kg/d for another 8 d. Mice that underwent BDL for 6 d and 14 d served as controls for the destruxin A5 treatment.

2.13. Statistical Analysis

All results shown represent means ± SEM. From triplicate experiments performed in a parallel manner. Data were statistically evaluated by one-way ANOVA followed by Dunnett's test between control group and multiple dose groups. The level of significance was set at a *P* value of 0.05.

3. Results

3.1. Destruxin A5 Inhibited PDGF-BB/PDGFR-ββ Signaling via a Different Mechanism than Tyrosine Kinase Inhibitors

To assess the influences of natural cyclopeptides including destruxin A5, trichomide C, roseocardin, homodestcardin, trichomide A, trichomide B, destruxin B and homodestruxin B (Fig. 1A and Supplementary Fig. 1) on PDGF-B/PDGFR-β signaling, the cellular expression levels of phosphorylated PDGFR-β, AKT and ERK were examined. Stimulation of the rat HSC line CFSC-8B with 10 ng/ml of PDGF-BB for 15–30 min led to the increased expression of p-PDGFR-β and its downstream signaling proteins, including p-AKT and p-ERK (Fig. 1B, C, and Supplementary Fig. 3). Western blotting also revealed that only destruxin A5 dose-dependently reduced the levels of p-PDGFR-β, p-AKT and p-ERK in PDGF-B-stimulated cells (Fig. 1B and C), whereas destruxin A5 had no effects on the phosphorylation of PDGFR-β, AKT and ERK in cells not stimulated with PDGF-B (Supplementary Fig. 2). Notably, destruxin A5 does not have the ability to bind to the ATP-binding pocket of tyrosine kinase domain when we tested the effect of destruxin A5 on the activated intracellular tyrosine kinase domain of human PDGFR-β (Fig. 1D). In contrast, sunitinib, which is a well-known tyrosine kinase inhibitor, displayed a very obvious inhibitory effect on the kinase activity of human PDGFR-β (Fig. 1D). Additionally, because no crystal structure of the intracellular tyrosine kinase domain of human PDGFR-β is available in the RCSB Protein Data Bank, we used a homology model/docking approach to measure the computational binding ability of destruxin A5 to the intracellular tyrosine kinase domain of human PDGFR-β using sunitinib as the positive control. According to the protocol published by Horbert, the *DFG-in* homology model of the intracellular tyrosine kinase domain was established using the crystal structure of VEGFR2 as the template (Horbert et al., 2015) (Supplementary Fig. 4A). Using the established model, the computational binding results from the AutoDock 4.2 software revealed that sunitinib exhibited a good affinity for the ATP-binding pocket of human PDGFR-β, and the modeled binding mode of sunitinib in PDGFR-β could be overlaid on its crystal structure form in VEGFR2 (Supplementary Fig. 4B), which suggests that this homology model could be used to test the computational binding ability of destruxin A5 to the ATP-binding pocket of human PDGFR-β. The calculated results indicated that destruxin A5 had no direct ligand-protein interaction with the ATP-binding pocket (data not shown), which is consistent with the kinase activity result.

3.2. Destruxin A5 was Able to Bind to the Extracellular Domain of Human PDGFR-β and Disrupt the Interaction Between PDGF-BB and PDGFR-β

To examine whether the extracellular domain of human PDGFR-β (Met 1-Lys 531) contained the binding site for destruxin A5, we used Biacore surface plasmon resonance (SPR), which is a novel and straightforward methodology for to study compound-protein interactions. Fig. 2A illustrates the binding of destruxin A5 to human PDGFR-β (Met 1-Lys 531), as captured on the sensor chip surface at 7200 relative units (RU). These results demonstrated that the responses observed for destruxin A5 correlated with its density. The rate constants of the Biacore T200 yielded an affinity for the destruxin A5/PDGFR-β interaction of 4.92 μM (Fig. 2A). Additionally, protein thermal shift technology and microscale thermophoresis technology were also used to strengthen the support for a destruxin A5/PDGFR-β interaction. These results indicated that destruxin A5 could bind to the extracellular domain of human PDGFR-β, leading to a protein thermal shift and a K_D value from the microscale thermophoresis of approximately 5.43 μM, which is consistent with the affinity yield by SPR (Supplementary Fig. 5). The reliability of Biacore's thermodynamic analysis has been confirmed in many studies (Bai et al., 2013; Papalia et al., 2008; Suzuki et al., 2009; Wear and Walkinshaw, 2006). Herein, the Biacore T200 technology was used to characterize the thermodynamic parameters of the binding of destruxin A5 to the extracellular domain of human PDGFR-β *via* conjunction with a Van't Hoff analysis (Supplementary Table 1). Analysis based on the Van't Hoff equation indicated that the thermodynamic parameters determined by SPR at 25 °C were as follows: $K_D \approx 8.02$ μM, $\Delta G^o \approx -6.95$ kcal·M^{-1}, $\Delta H^o \approx -2.28$ kcal·M^{-1}, $T\Delta S^o \approx 4.66$ kcal·M^{-1} and $\Delta C_P \approx 1.04$ kcal·K^{-1}·M^{-1}. These findings also indicated that destruxin A5 was able to bind to the extracellular domain of human PDGFR-β. Additionally, the SPR results indicated that the other natural cyclopeptides evaluated in this study minimally bound to

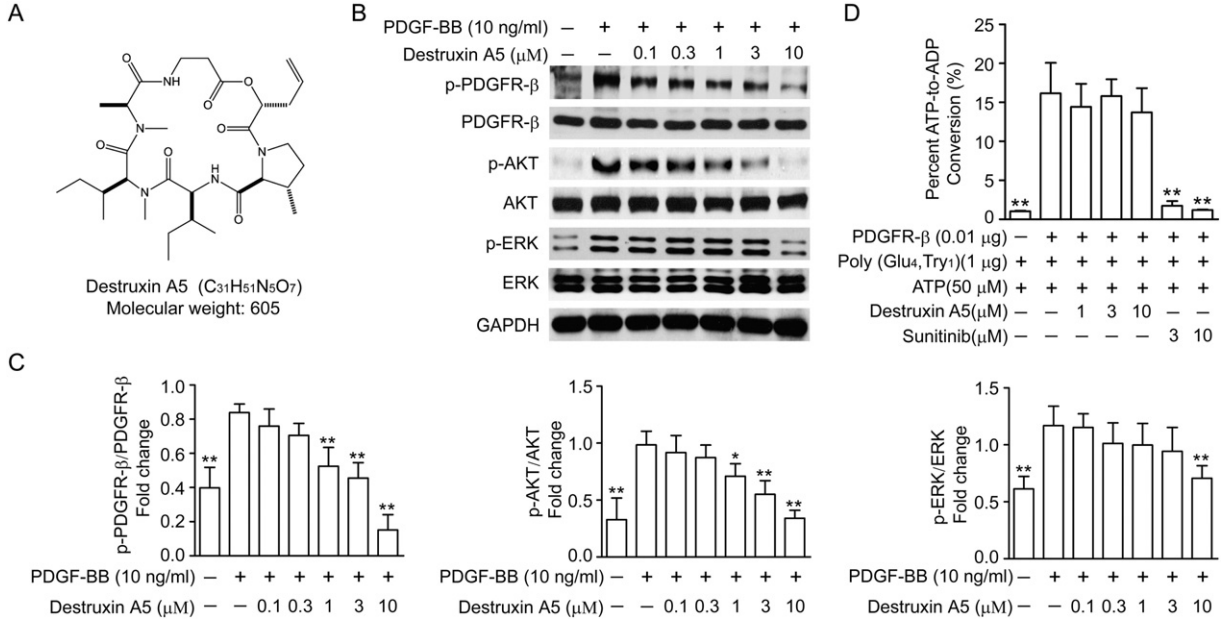

Fig. 1. PDGF-BB/PDGFR-ββ signaling was inhibited by destruxin A5. (A) The chemical structure of destruxin A5. (B and C) Representative western blot bands and a data summary (n = 4 each group) of expression of PDGF-BB/PDGFR-ββ signaling-related proteins. The western blotting data are presented as the means ± SEM. (D) The effect of destruxin A5 on human PDGFR-β activity was determined using the PDGFR-β activity assay kit (n = 6 each group). The data are expressed as histogram containing the means ± SEM. of three independent experiments. $^*P < 0.05$, $^{**}P < 0.01$ versus the control group.

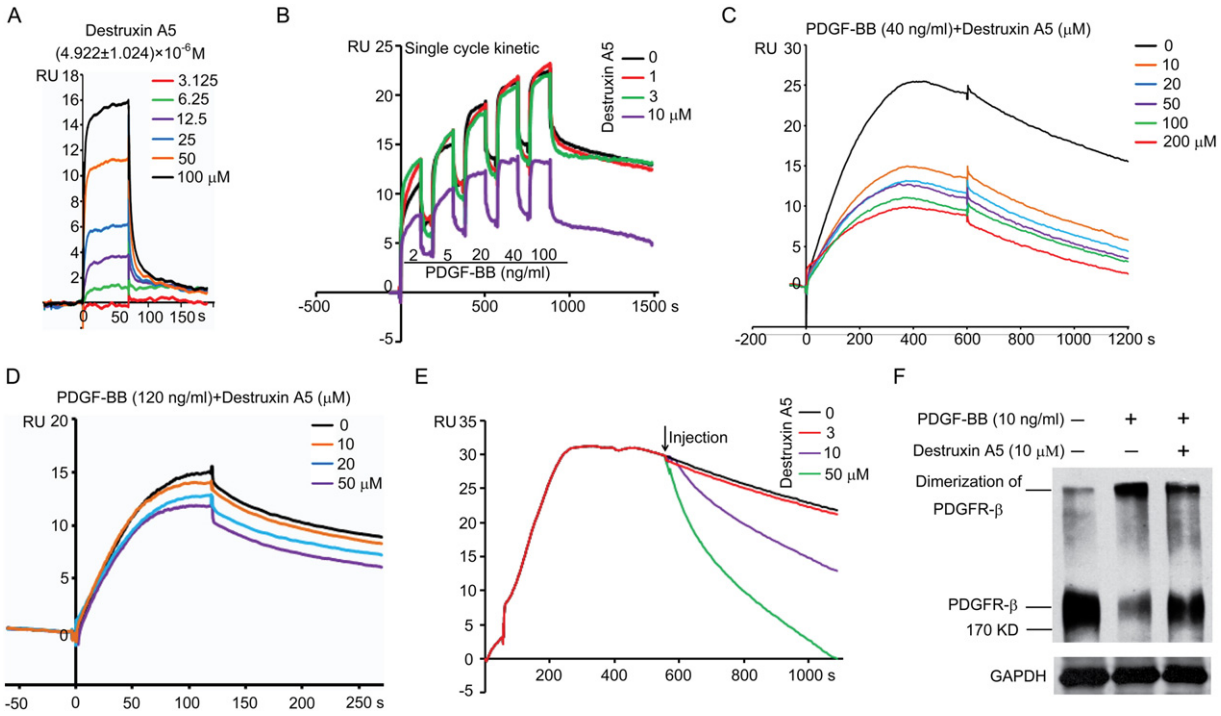

Fig. 2. Destruxin A5 bound to human PDGFR-β (Met 1-Lys 531) protein and blocked the interaction between PDGF-BB and PDGFR-β. (A) Destruxin A5 associated with human PDGFR-β (Met 1-Lys 531) protein as measured by SPR analysis. (B) The inhibitory effect of destruxin A5 on the PDGF-B/PDGFR-β interaction was evaluated using the single-cycle kinetic methodology of SPR. (C and D) Destruxin A5 blocked the interaction between PDGF-BB and PDGFR-β, as measured with SPR. (E) Destruxin A5 promoted the dissociation of PDGF-BB from PDGFR-β. (F) Destruxin A5 blocked PDGFR-β dimerization induced by PDGF-BB in the cellular system, as measured by non-denaturing western blotting. The data represented here represent one of three independent experiments with similar results.

PDGFR-β (Met 1-Lys 531) (Supplementary Fig. 6). Moreover, destruxin A5 was unable to interact with PDGF-B (Supplementary Fig. 7). Using the single-cycle kinetic methodology of the Biacore T200 to test the influence of destruxin A5 on the PDGF-BB/PDGFR-β interaction, we found that the response of PDGF-BB to PDGFR-β was markedly decreased by destruxin A5 at 10 μM (Fig. 2B). When we measured the responses of admixtures (40 ng/ml PDGF-BB with different concentrations of destruxin A5) to PDGFR-β, the response values were found to be significantly reduced by destruxin A5 in a dose-dependent manner compared with the only PDGF-BB group, and the inhibitory effect of destruxin A5 was weakened by the 3-fold higher concentration of PDGF-BB (Fig. 2C and D). In addition to the inhibitory effect of destruxin A5 on the binding process of PDGF-BB to PDGFR-β, destruxin A5 (10 and 50 μM) also promoted the dissociation of PDGF-BB from PDGFR-β (Fig. 2E). It is also known that PDGF-BB can enhance the conformation of PDGFR-ββ (Bonner, 2004; Shim et al., 2010). Accordingly, non-denaturing western blotting revealed that the PDGF-BB-induced PDGFR-β dimerization (PDGFR-ββ) in cultured HSCs was blocked by destruxin A5, which further confirmed the SPR results in our cellular system (Fig. 2F).

3.3. Destruxin A5 Selectively Blocked PDGF-BB/PDGFR-ββ Signaling by Targeting and Occupying the Binding Sites of PDGF-B with PDGFR-β

To identify the site in the extracellular domain of human PDGFR-β to which destruxin A5 bound, we created a series of amino acid mutations in the human PDGFR-β protein based on the binding amino acids of the PDGF-B/PDGFR-β interface. We filtered the affinities of destruxin A5 to different mutated human PDGFR-β proteins using Biacore's SPR methodology. The SPR results demonstrated that the K_D value of the Phe136/Ala136 and Phe138/Ala138 mutated group was 99.5 μM, which was approximately 20.2-fold higher than that of the wild-type human PDGFR-β protein (Fig. 3A). This result indicated that Phe136 and Phe138 in human PDGFR-β contribute to the affinity of the destruxin A5/PDGFR-β interaction and that the binding sites of destruxin A5 in human PDGFR-β were the sites of the binding of PDGF-B. PDGF-B was able to firmly bind to wild-type PDGFR-β (Fig. 3B), whereas it minimally bound to Phe136/Ala136 and Phe138/Ala138 mutated forms of PDGFR-β (Fig. 3C), which revealed that mutations in Phe136 and Phe138 could strongly influence the PDGF-B/PDGFR-β interaction. Additionally, analysis with the AutoDock 4.2 software also indicated interactions between destruxin A5 and amino acids, including Phe136 and Phe138 (Fig. 3D). Notably, the inhibitory effect of destruxin A5 on PDGF-BB/PDGFR-ββ signaling was not related to PDGFR-β endocytosis because destruxin A5 induced minimal PDGFR-β endocytosis in CFSC-8B cells, as measured with flow cytometry and western blotting (Supplementary Fig. 8). Importantly, destruxin A5 exhibited no abilities to bind to the extracellular domains of human PDGFR-α, VEGFR1, VEGFR2, FLT3, KIT, EGFR or IFN-γR1 (Fig. 4). Furthermore, destruxin A5 exhibited an inhibitory effect on the growth of PDGF-BB-stimulated HepG-2 cells and OS-RC-2 cells, with sunitinib as the positive control (Supplementary Fig. 9). However, destruxin A5 minimally inhibited the cell proliferation induced by PDGF-AA, VEGF, FLT3 ligand and KIT ligand (Supplementary Fig. 10).

3.4. Destruxin A5 Suppressed PDGF-BB-induced HSC Activation, Proliferation, Migration, Cell Cycle Progression and Fibrosis-related Protein Expression In Vitro

To observe the effects of destruxin A5 on PDGF-BB/PDGFR-ββ signaling in a cellular system, cell activation, proliferation, migration, cell cycle progression and fibrosis-related protein expression were examined in our study. As shown in Fig. 5A, destruxin A5 exhibited a minimal effect on cell viability in PDGFR-β low-expressed LX-2 cells during their quiescent phase (cultured LX-2 cells were quiescent during the first 3 d of culture (Li et al., 2014)). However, destruxin A5 dose-dependently inhibited the proliferation of PDGF-BB-activated LX-2 cells and PDGF-BB-stimulated CFSC-8B cells (Fig. 5B–D). HSCs can migrate in response to PDGF-BB stimuli (Patsenker et al., 2007). Not only cell proliferation

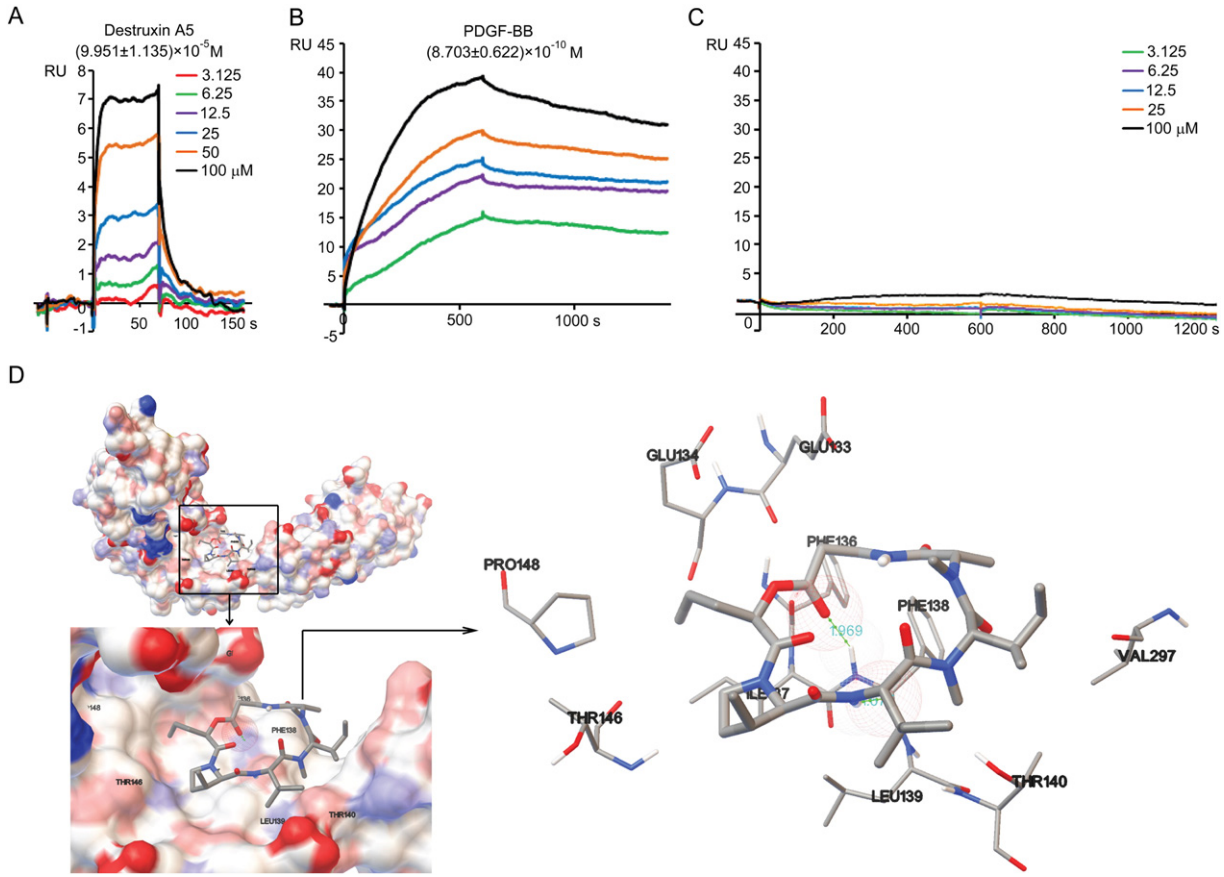

Fig. 3. Destruxin A5 occupied the interface between PDGF-BB and PDGFR-β. (A) The binding abilities of destruxin A5 to human PDGFR-β (Met 1-Lys 531) proteins with the Phe136/Ala136 and Phe138/Ala138 mutations were measured by SPR. (B and C) PDGF-BB associated with human PDGFR-β (Met 1-Lys 531) protein with or without the Phe136/Ala136 and Phe138/Ala138 mutations, as measured with SPR. (D) The computational binding mode of destruxin A5 in human PDGFR-β was established using AutoDock 4.2 software. The data represented here represent one of three independent experiments with similar results.

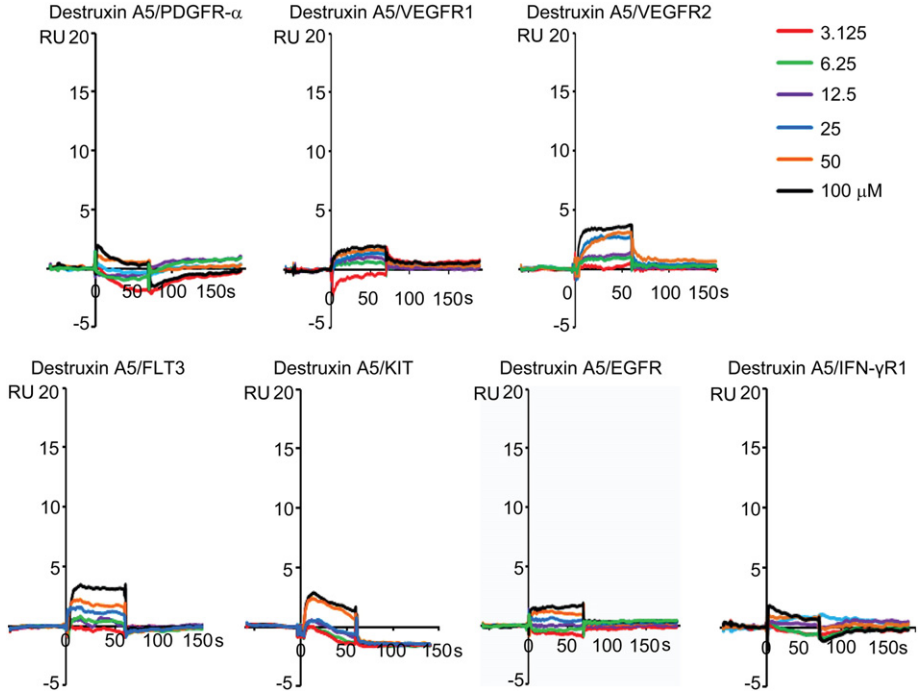

Fig. 4. Destruxin A5 was unable to bind to the extracellular domains of human PDGFR-α, VEGFR1, VEGFR2, FLT3, KIT, EGFR or IFN-γR1. The binding abilities of destruxin A5 to the extracellular domains of human PDGFR-α, VEGFR1, VEGFR2, FLT3, KIT, EGFR and IFN-γR1 were measured by SPR. The responses of destruxin A5 to these proteins were very weak, which indicated that destruxin A5 did not directly interact with these proteins. The data represented here represent one of three independent experiments with similar results.

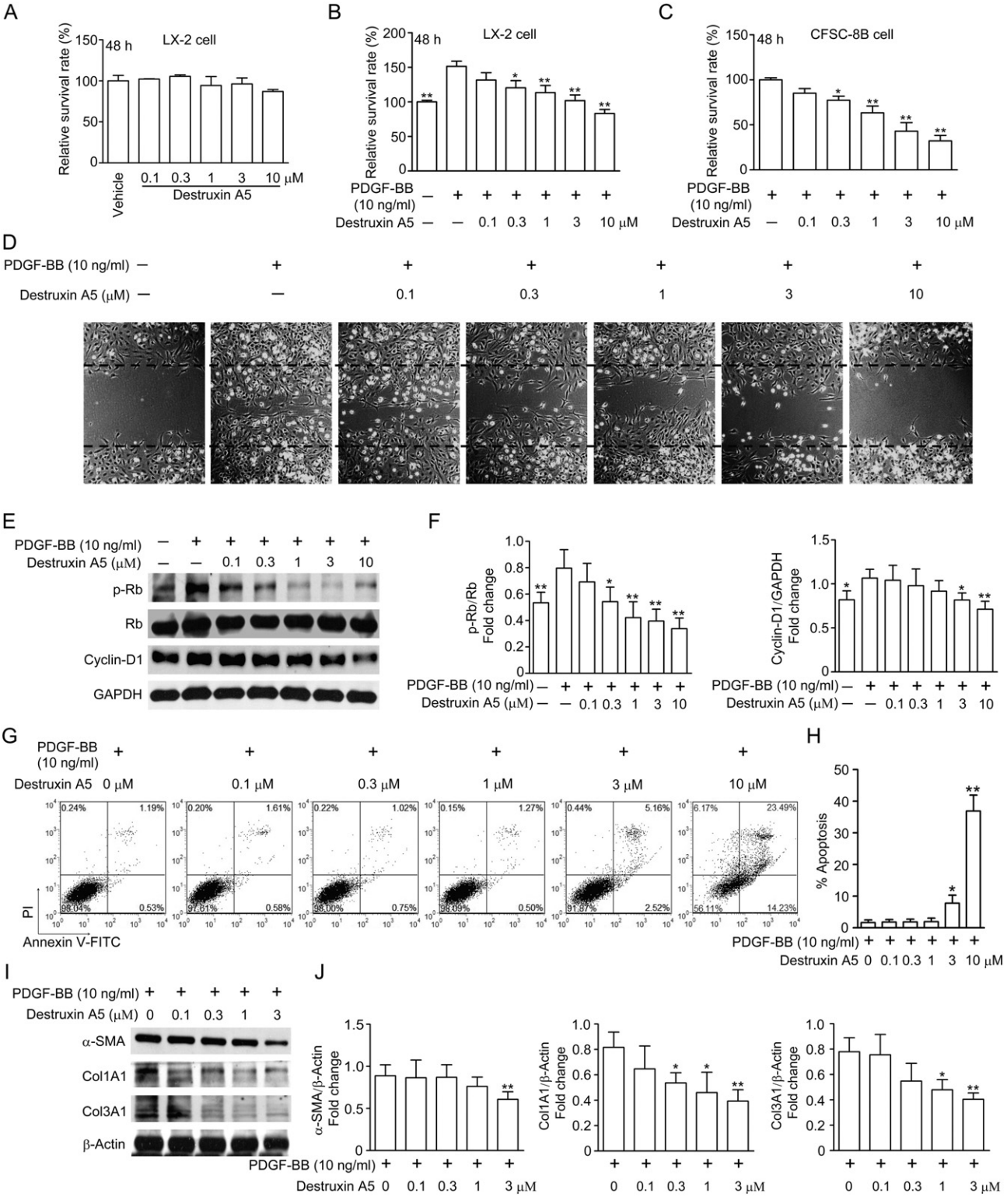

Fig. 5. Destruxin A5 promoted antifibrotic effects *in vitro*. (A) The effect of destruxin A5 on the survival of quiescent LX-2 cells was assessed with the MTT assay (n = 8 each group). The cell proliferation-inhibiting effects of destruxin A5 on PDGF-BB-activated LX-2 cells (n = 8 each group) (B) and CFSC-8B cells (n = 8 each group) (C) were evaluated using MTT assays. (D) The effects of destruxin A5 on CFSC-8B migration induced by PDGF-BB were appraised according to the linear wound repair capacity. (E and F) Representative western blot bands and a data summary (n = 4 each group) of expression of cycle-related proteins. These proteins in CFSC-8B cells were down-regulated by destruxin A5. (G and H) Destruxin A5 induced apoptosis in CFSC-8B cells (n = 4 each group). (I and J) Representative western blot bands and a data summary (n = 4 each group) of expression of α-SMA, Col1A1 and Col3A1. These proteins in CFSC-8B cells were decreased by destruxin A5. The data are expressed as a histogram illustrating the means ± SEM. of three independent experiments. $^{*}P < 0.05$, $^{**}P < 0.01$ *versus* the control group.

but also cell migration can be tested by wound healing assay (Fig. 5D). PDGF-BB enhanced the migration of HSCs to repair linear wounds created in cultured CFSC-8B cells (Fig. 5D). However, destruxin A5 effectively prevented the migration of HSCs via the blockade of PDGF-BB/PDGFR-ββ signaling (Fig. 5D). Using other cell lines to confirm the inhibitory effect of destruxin A5 on migration, the suppression of wound repair and

cell invasion was also observed in PDGF-BB-treated OS-RC-2 cells (Supplementary Fig. 11). However, the other natural cyclopeptides were unable to block PDGF-BB/PDGFR-ββ signaling and minimally inhibited CFSC-8B cell migration (Supplementary Fig. 12). PDGF-BB stimulated cell cycle progression in LX-2 cells, which was blocked by destruxin A5 in a concentration-dependent manner (Supplementary Fig. 13); this effect was also blocked in the PDGF-BB-treated OS-RC-2 cells (Supplementary Fig. 14). Additionally, the expression levels of cell cycle proteins, including p-Rb and Cyclin-D1, were reduced by destruxin A5 treatment (Fig. 5E and F). Moreover, destruxin A5 increased apoptosis (Fig. 5G and H) and decreased the protein expression of liver fibrosis-related α-SMA, Col1A1 and Col3A1 in PDGF-BB-activated HSCs (Fig. 5I and J).

3.5. Destruxin A5 Attenuated Bile Duct Ligation (BDL)-induced Liver Fibrosis by Blocking PDGF-BB/PDGFR-ββ Signaling

Next, we verified the unique inhibitory effect of destruxin A5 on PDGF-BB/PDGFR-ββ signaling *in vivo*. Six days after BDL surgery, liver injury and fibrosis were observed in operated mice. These conditions became more severe in the subsequent 8 d of BDL, as confirmed by hematoxylin–eosin staining, Masson trichrome staining and immunohistochemistry (Fig. 6A–C and Supplementary Fig. 15). However, the therapeutic administration of destruxin A5 clearly ameliorated the liver injury and reduced the accumulation of fibrosis (Fig. 6A, B and Supplementary Fig. 15). The anti-fibrotic property of destruxin A5 in BDL-treated mice was further verified by evaluating the effect of destruxin A5 on α-SMA protein expression using immunohistochemistry (Fig. 6C). The therapeutic administration of destruxin A5 markedly mitigated the expression of α-SMA in BDL-induced liver fibrosis compared with the control group (Fig. 6C). Additionally, we assessed the spleen weight/body weight ratio, content of hydroxyproline, serum total bilirubin, and serum alanine aminotransferase (ALT) and aspartate aminotransferase (AST) levels to provide further evidence of the anti-fibrotic properties of destruxin A5 in BDL-treated mice (Fig. 6D). As shown in Fig. 6D, the spleen values were dramatically decreased in animals with experimental liver fibrosis following therapeutic treatment with destruxin A5, and the hydroxyproline content was also reduced in BDL-treated mice after therapeutic destruxin A5 treatment. Additionally, the levels of serum total bilirubin, ALT and AST were also evidently decreased after the therapeutic administration of destruxin A5 to animals with BDL-induced liver fibrosis (Fig. 6D). To further explore the mechanism by which destruxin A5 improved the BDL-induced liver fibrosis, we accessed the expression of PDGFR-β, p-PDGFR-β, PDGFR-α, p-AKT, p-ERK, α-SMA and PDGF-BB in the fibrotic livers. Immunohistochemical examination revealed that the protein expression

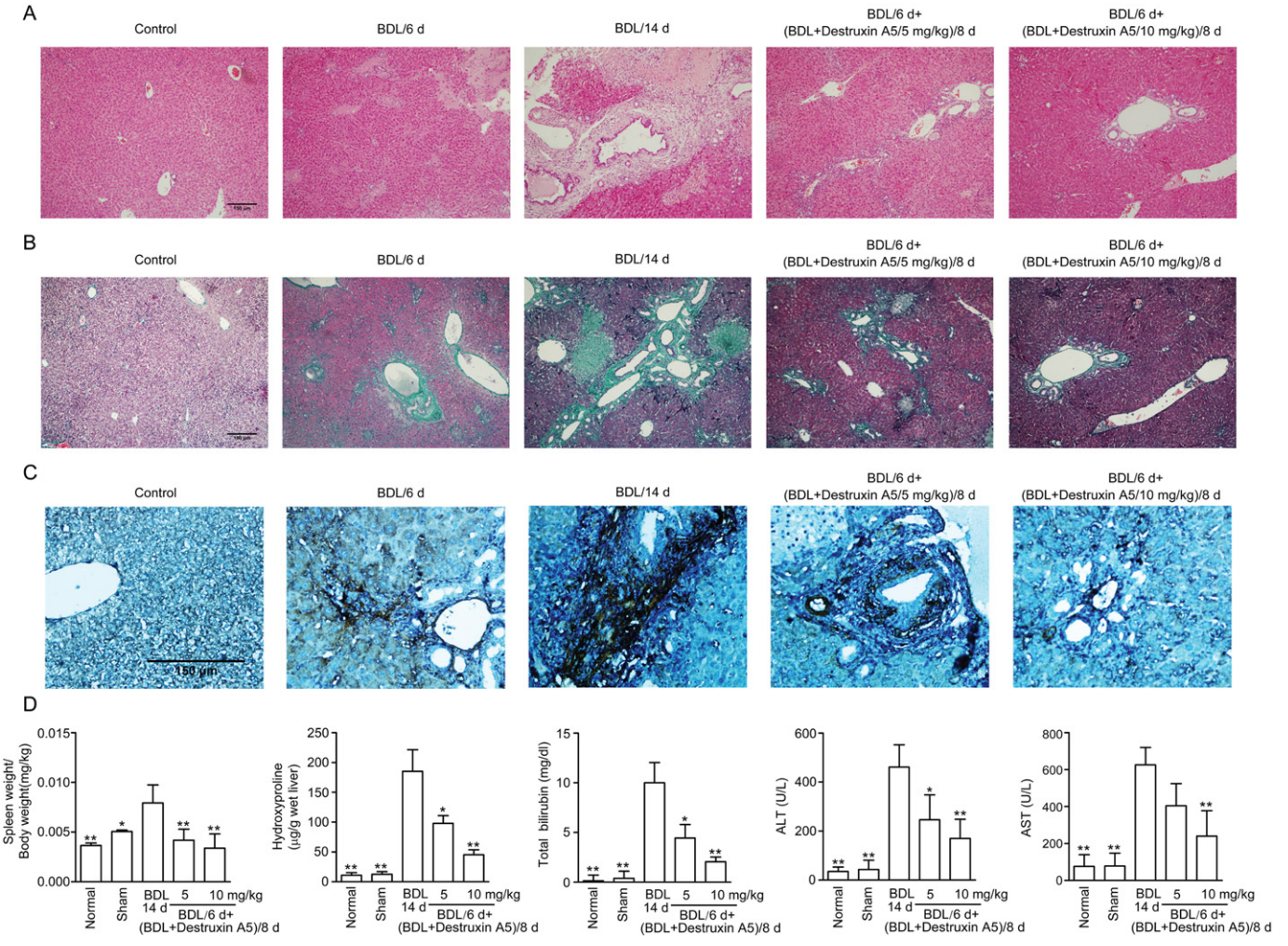

Fig. 6. Destruxin A5 mitigated BDL-induced liver fibrosis in mice (n = 8 in each group). (A) Effects of destruxin A5 on liver fibrosis in BDL mice. Sections of mouse liver were stained with hematoxylin–eosin and examined by a blinded histologist (original magnification × 200). (B) Effect of destruxin A5 on collagen expression in mice with liver fibrosis. Liver sections were stained with Masson and examined by a blinded histologist (original magnification × 200). (C) Effect of destruxin A5 on α-SMA expression in mice with liver fibrosis. Hepatic immunohistochemical staining with α-SMA. The data represented here represent one of three independent experiments with similar results. (D) The spleen index, liver hydroxyproline content, total bilirubin content in serum, ALT content in serum and AST content in serum were tested in this study. The data are expressed as histograms illustrating the means ± the SEM. of three independent experiments. $^{*}P < 0.05$, $^{**}P < 0.01$ *versus* the BDL 14 d group.

of p-PDGFR-β was significantly increased in BDL-treated mice, whereas this expression was suppressed by destruxin A5 therapeutic treatment (Fig. 7A). The western blot results demonstrated that PDGFR-β expression was highly induced in fibrotic livers, whereas PDGFR-α was constitutively expressed in the normal livers and fibrotic livers. Additionally, the phosphorylation of PDGF-BB/PDGFR-ββ signaling-associated proteins, including PDGFR-β, AKT and ERK, was down-regulated by therapeutic treatment with destruxin A5. The expression level of α-SMA was also decreased by destruxin A5, although this therapeutic treatment was unable to reduce the level of PDGF-BB in BDL-induced fibrotic livers (Fig. 7B and C). In addition to the *in vivo* examination, we used precision-cut liver slices and a well-known tissue model for the early onset of liver fibrosis to test the efficacies of antifibrotic drugs (Westra et al., 2014) and to evaluate the inhibitory effects of destruxin A5 on PDGF-BB/PDGFR-ββ signaling. The q-PCR results revealed that the mRNA levels of α-SMA, Col1A1 and HSP47 in the liver slices were increased by PDGF-BB treatment but decreased by destruxin A5 (Supplementary Fig. 16).

3.6. p-PDGFR-β was Expressed in the Liver Tissues of Patients with Cirrhosis

Hepatitis B virus (HBV) can cause chronic liver injury resulting in liver fibrosis, and the end stage consequence of liver fibrosis is liver cirrhosis (Bataller and Brenner, 2005; Bonner, 2004; Kocabayoglu et al., 2015). To test whether phosphorylated PDGFR-β is expressed in hepatic tissue with cirrhosis, cirrhotic liver samples were obtained from 62 HBV-positive patients, and samples from 35 human normal controls were used as the control group. The immunohistochemistry results revealed that the 37 cirrhotic liver samples expressed p-PDGFR-β in the fibrotic areas, whereas the normal hepatic tissue samples

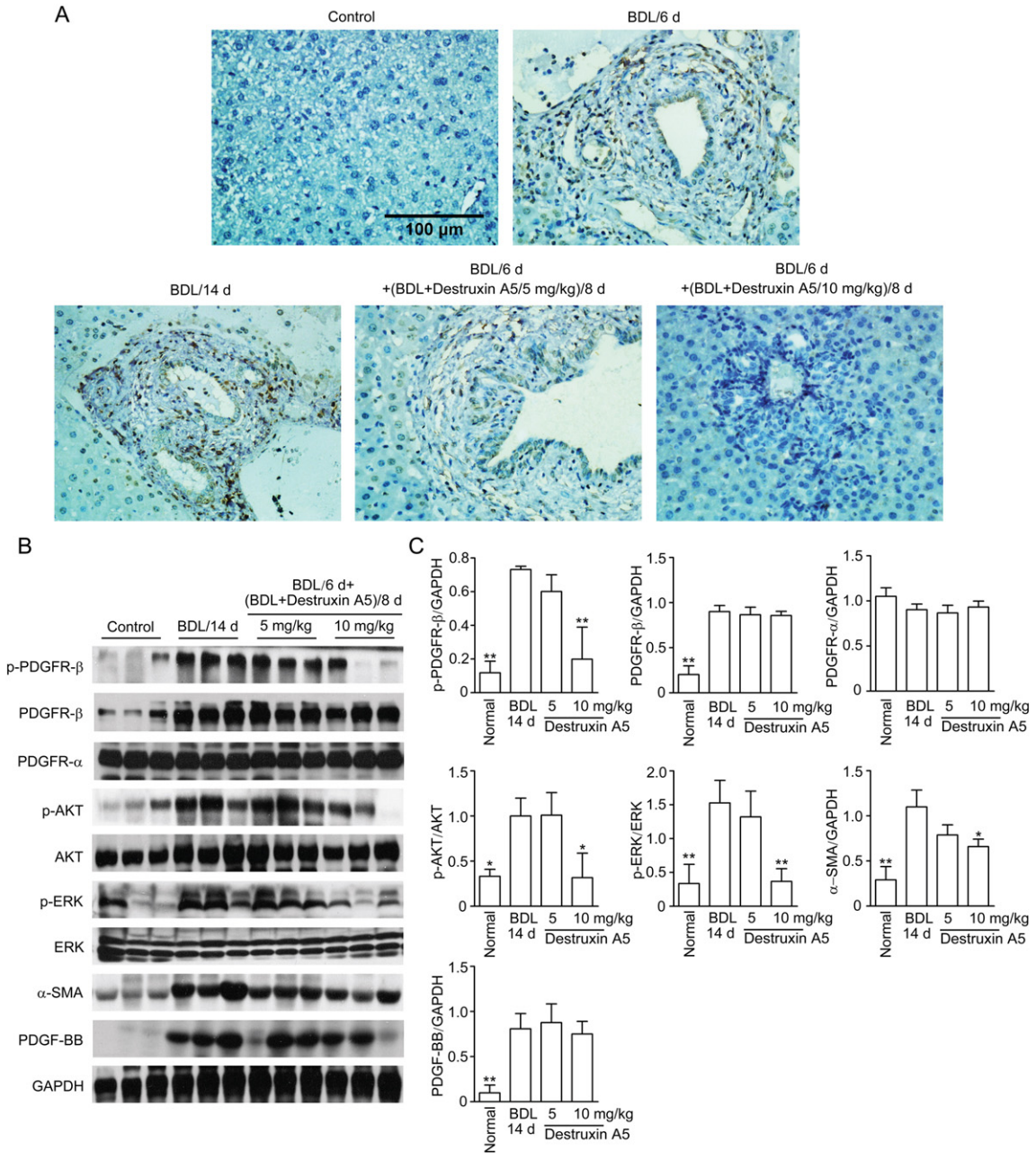

Fig. 7. Effects of destruxin A5 on the expression of p-PDGFR-β, PDGFR-β, PDGFR-α, p-Akt, Akt, p-ERK, ERK, α-SMA, PDGF-BB and GAPDH in the livers of mice with liver fibrosis induced by BDL (n = 8 in each group). (A) Hepatic immunohistochemical staining with p-PDGFR-β antibody. The data represented here represent one of three independent experiments with similar results. (B and C) Total lysates from liver specimens of the control and destruxin A5-treated groups were subjected to western blot analysis. The data are expressed as histograms illustrating the means ± SEM. of three independent experiments. $^{*}P < 0.05$, $^{**}P < 0.01$ *versus* the BDL 14 d group.

expressed minimal p-PDGFR-β (Fig. 8), which indicated that p-PDGFR-β-positive cells may represent an important hallmark and therapeutic target for liver fibrosis.

4. Discussion

PDGF-BB/PDGFR-ββ signaling is a druggable target whose inhibition mitigates liver fibrosis severity (Liu et al., 2011). Several strategies to block PDGF-BB/PDGFR-ββ signaling have been applied in scientific research on liver fibrosis. For instance, PDGF-B monoclonal antibody, adenoviral dominant-negative soluble PDGFR-β and HSCs-specific PDGFR-β small interference RNA have been developed to inhibit PDGF-BB/PDGFR-ββ signaling to ameliorate liver fibrosis in rodent disease models (Chen et al., 2008; Reichenbach et al., 2012; Yoshida et al., 2014). Currently approved medical therapies acting through PDGF-BB/PDGFR-ββ inhibition are based on multi-targeting tyrosine-kinase inhibitors (Ehnman and Östman, 2014; Grassot et al., 2006; Horbert et al., 2015; Westra et al., 2014). Although monoclonal antibodies possess a selective affinity for their target, they also have limitations (Miller et al., 2013; Mócsai et al., 2014). Small-molecule inhibitors offer unique advantages, but they are usually nonselective or less selective (Ehnman and Östman, 2014; Horbert et al., 2015; Mócsai et al., 2014). Thus, the identification or design of small-molecule inhibitors with increased selective affinity to PDGFR-β represents an active area of research.

Notably, every tyrosine kinase receptor has a unique extracellular domain for its own ligand, which constitutes a distinct protein–protein interaction interface between a ligand and its tyrosine kinase receptor. If we could identify a small-molecule compound that targets the PDGF-B/PDGFR-β interaction interface, it may serve as a selective inhibitor of PDGFR-β. However, modulating protein–protein interactions with small organic compounds remains enormously challenging because the interface areas are typically large (generally, an average interface area is close to 1150–10,000 Å^2) and flat (Ivanov et al., 2013). Additionally, the interface areas are typically hydrophobic and often lack the deep grooves that provide an interface for small molecule docking (Ivanov et al., 2013). Utilizing the proangiogenic VEGF/VEGFR protein–protein interface (Gautier et al., 2011) and the oncogenic ERK/ERK protein–protein interface (Herrero et al., 2015), researchers have found drug-like small molecules using structure-based screening, which could specifically inhibit the formation of the VEGFR1/VEGF complex and the dimeric ERK/ERK complex (Gautier et al., 2011; Herrero et al., 2015). These successful reports inspired us to search for a more selective inhibitor of PDGFR-β based on the PDGF-B/PDGFR-β interaction interface.

Fortunately, we found that destruxin A5, a natural cyclopeptide, had the ability to block PDGF-BB/PDGFR-ββ signaling without binding to the ATP-binding pocket of human PDGFR-β, as observed with tyrosine kinase inhibitors (Fig. 1). This interesting and puzzling phenomenon attracted our attention. Surprisingly, destruxin A5 was able to bind to the extracellular domain of human PDGFR-β but did not directly interact with PDGF-BB (Fig. 2, Supplementary Fig. 5 and Supplementary Fig. 7). Importantly, destruxin A5 was able to block the interaction between PDGF-B and PDGFR-β and inhibit the dimerization of PDGFR-β that is induced by PDGF-BB stimulation of HSCs (Fig. 2), which indicated that the initiation of PDGF-B/PDGFR-ββ signaling was blocked by destruxin A5. We were also eager to explore the mechanism by which destruxin A5 was able to block the PDGF-B/PDGFR-β interaction. Encouragingly, our results suggested that destruxin A5 binds to human PDGFR-β via interactions with Phe136 and Phe138 (Fig. 3). It should

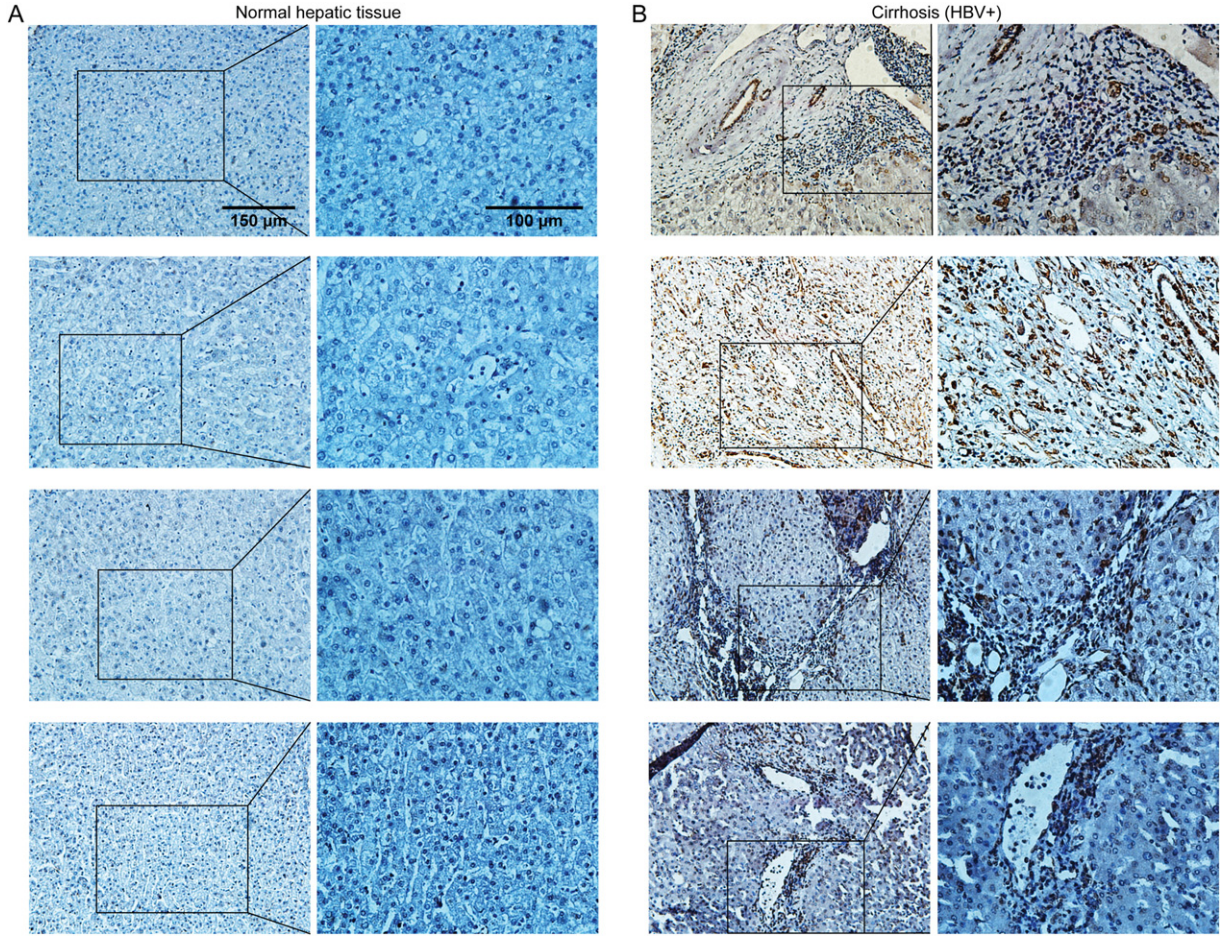

Fig. 8. The expression of p-PDGFR-β in cirrhotic liver samples from 62 HBV-positive patients and 35 normal controls was evaluated using tissue microarray. Hepatic immunohistochemical staining with p-PDGFR-β antibody, (A) Representative staining from normal controls, and (B) cirrhotic liver samples.

be emphasized that the PDGF-B/PDGFR-β interface is formed by the side chains of Phe136, Phe138, Tyr205, Tyr207 from PDGFR-β and Leu38, Trp40, Ile75, Ile77, Pro82, Phe84 from PDGF-B (Shim et al., 2010). Additionally, the PDGFR-β sequences were highly conserved among mouse, rat and human (Supplementary Fig. 17). The overall PDGFR-β sequence similarity of mouse or rat with human PDGFR-β sequence was 92% and between mouse and rat 98%. Importantly, the PDGFR-β sequences of mouse, rat and human all contain Phe136, Phe138, Tyr205 and Tyr207. These data demonstrate that destruxin A5 is a compound that targets the PDGF-B/PDGFR-β interaction interface to block PDGF-BB/PDGFR-ββ signaling in mouse, rat and human. In the current study, one of our most important finding was the selective inhibitory property of destruxin A5 for PDGF-BB/PDGFR-ββ signaling, as destruxin A5 elicited no inhibitory effect on the kinase activity of the tyrosine kinase and had no direct effects on the interactions with the extracellular domains of human PDGFR-α, VEGFR1, VEGFR2, FLT3, KIT, EGFR or IFN-γR1 (Fig. 4), Moreover, destruxin A5 only slightly inhibited the cell proliferation induced by PDGF-AA, VEGF, FLT3 ligand and KIT ligand, whereas the cell proliferation induced by PDGF-BB was dose-dependently suppressed by destruxin A5 (Supplementary Fig. 9 and Supplementary Fig. 10). Thus, our study confirms the selective inhibitory effect of destruxin A5 on PDGF-BB/PDGFR-ββ signaling. These findings may confer substantial benefits to liver fibrosis patients. Indeed, our *in vitro* studies validated the suppressive effect of destruxin A5 on PDGF-BB/PDGFR-ββ signaling-mediated activation, proliferation, migration, cell cycle progression and fibrosis-related protein expression in HSCs (Fig. 5). Apoptosis is an important mechanism to reduce the number of activated HSCs (Liu et al., 2011). Thus, we evaluated the effect of destruxin A5 on apoptosis and found that destruxin A5 significantly increased the level of apoptosis in activated HSCs (Fig. 5G and H). Moreover, the antifibrotic effects of destruxin A5 on liver fibrosis were verified in *ex vivo* and *in vivo* models, and the mechanism underlying the antifibrotic effect of destruxin A5 was shown to be due to its selective inhibitory role in PDGF-BB/PDGFR-ββ signaling (Figs. 6, 7 and Supplementary Fig. 16). Importantly, the unique therapeutic effect of destruxin A5 on liver fibrosis carries extremely important and potential clinical significance because p-PDGFR-β is wildly expressed in cirrhotic liver tissues from HBV-positive patients (Fig. 8).

PDGF-BB/PDGFR-ββ signaling represents a key target for the treatment of liver fibrosis, and destruxin A5 is a small-molecule inhibitor shown to possess efficacious and more selective properties for this crucial pathogenic component of liver fibrosis. Additionally, destruxin A5 could also be used in the treatment of other PDGFR-β-related diseases, such as cancer. Together, our results stimulate further interest in the identification of small-molecule compounds that possess more selective affinity for single cell surface tyrosine kinase receptors.

Conflicts of Interest

The authors have no competing interests to declare.

Author Contributions

X.Q.W. conceived and designed the studies, performed experiments, analyzed data, and wrote the manuscript. A.H.Z., S.Y.W., C.H.H. and W.C. performed experiments. Y.S., R.X.T. and Y.S. conceived and designed the studies, and contributed to statistical analyses. X.F.W. and Q.X. conceived and designed the studies, and contributed to the writing of the manuscript.

Acknowledgments

This work was supported by National Natural Science Foundation of China (Nos. 91313303, 81373466, 81422050) and Natural Science Foundation of Jiangsu Province (BK20151394).

Appendix A. Supplementary data

Supplementary data to this article can be found online at http://dx.doi.org/10.1016/j.ebiom.2016.03.042.

References

Andrae, J., Gallini, R., Betsholtz, C., 2008. Role of platelet-derived growth factors in physiology and medicine. Genes Dev. 22, 1276–1312.
Arora, A., Scholar, E.M., 2005. Role of tyrosine kinase inhibitors in cancer therapy. J. Pharmacol. Exp. Ther. 315, 971–979.
Bai, F., Xu, Y., Chen, J., Liu, Q., Gu, J., Wang, X., Ma, J., Li, H., Onuchic, J.N., Jiang, H., 2013. Free energy landscape for the binding process of Huperzine A to acetylcholinesterase. Proc. Natl. Acad. Sci. U. S. A. 110, 4273–4278.
Bansal, R., Prakash, J., Post, E., Beljaars, L., Schuppan, D., Poelstra, K., 2011. Novel engineered targeted interferon-gamma blocks hepatic fibrogenesis in mice. Hepatology 54, 586–596.
Bansal, R., Prakash, J., De Ruiter, M., Poelstra, K., 2014. Interferon gamma peptidomimetic targeted to hepatic stellate cells ameliorates acute and chronic liver fibrosis in vivo. J. Control. Release 179, 18–24.
Bataller, R., Brenner, D.A., 2005. Liver fibrosis. J. Clin. Invest. 115, 209–218.
Beljaars, L., Weert, B., Geerts, A., Meijer, D.K., Poelstra, K., 2003. The preferential homing of a platelet derived growth factor receptor-recognizing macromolecule to fibroblast-like cells in fibrotic tissue. Biochem. Pharmacol. 66, 1307–1317.
Bonner, J.C., 2004. Regulation of PDGF and its receptors in fibrotic diseases. Cytokine Growth Factor Rev. 15, 255–273.
Borkham-Kamphorst, E., Meurer, S.K., Van de Leur, E., Haas, U., Tihaa, L., Weiskirchen, R., 2015. PDGF-D signaling in portal myofibroblasts and hepatic stellate cells proves identical to PDGF-B via both PDGF receptor type α and β. Cell. Signal. 27, 1305–1314.
Brennand, D.M., Scully, M.F., Kakkar, V.V., Patel, G., 1997. A cyclic peptide analogue of loop III of PDGF-BB causes apoptosis in human fibroblasts. FEBS Lett. 419, 166–170.
Chen, S.W., Chen, Y.X., Zhang, X.R., Qian, H., Chen, W.Z., Xie, W.F., 2008. Targeted inhibition of platelet-derived growth factor receptor-beta subunit in hepatic stellate cells ameliorates hepatic fibrosis in rats. Gene Ther. 15, 1424–1435.
Ehnman, M., Östman, A., 2014. Therapeutic targeting of platelet-derived growth factor receptors in solid tumors. Expert Opin. Investig. Drugs 23, 211–226.
Gautier, B., Miteva, M.A., Goncalves, V., Huguenot, F., Coric, P., Bouaziz, S., Seijo, B., Gaucher, J.F., Broutin, I., Garbay, C., et al., 2011. Targeting the proangiogenic VEGF-VEGFR protein–protein interface with drug-like compounds by in silico and in vitro screening. Chem. Biol. 18, 1631–1639.
Grassot, J., Gouy, M., Perrière, G., Mouchiroud, G., 2006. Origin and molecular evolution of receptor tyrosine kinases with immunoglobulin-like domains. Mol. Biol. Evol. 23, 1232–1241.
Herrero, A., Pinto, A., Colón-Bolea, P., Casar, B., Jones, M., Agudo-Ibáñez, L., Vidal, R., Tenbaum, S.P., Nuciforo, P., Valdizán, E.M., et al., 2015. Small molecule inhibition of ERK dimerization prevents tumorigenesis by RAS–ERK pathway oncogenes. Cancer Cell 28, 170–182.
Horbert, R., Pinchuk, B., Johannes, E., Schlosser, J., Schmidt, D., Cappel, D., Totzke, F., Schächtele, C., Peifer, C., 2015. Optimization of potent DFG-in inhibitors of platelet derived growth factor receptorβ (PDGF-Rβ) guided by water thermodynamics. J. Med. Chem. 58, 170–182.
Ivanov, A.A., Khuri, F.R., Fu, H., 2013. Targeting protein–protein interactions as an anticancer strategy. Trends Pharmacol. Sci. 34, 393–400.
Kocabayoglu, P., Lade, A., Lee, Y.A., Dragomir, A.C., Sun, X., Fiel, M.I., Thung, S., Aloman, C., Soriano, P., Hoshida, Y., et al., 2015. β-PDGF receptor expressed by hepatic stellate cells regulates fibrosis in murine liver injury, but not carcinogenesis. J. Hepatol. 63, 141–147.
Kondo, R., Yano, H., Nakashima, O., Tanikawa, K., Nomura, Y., Kage, M., 2013. Accumulation of platelets in the liver may be an important contributory factor to thrombocytopenia and liver fibrosis in chronic hepatitis C. J. Gastroenterol. 48, 526–534.
Krasnoff, S.B., Gibson, D.M., Belofsky, G.N., Gloer, K.B., Gloer, J.B., 1996. New Destruxins from the Entomopathogenic Fungus Aschersonia sp. J. Nat. Prod. 59, 485–489.
Li, Z.J., Ou-Yang, P.H., Han, X.P., 2014. Profibrotic effect of miR-33a with Akt activation in hepatic stellate cells. Cell. Signal. 26, 141–148.
Liu, Y., Wang, Z., Kwong, S.Q., Lui, E.L., Friedman, S.L., Li, F.R., Lam, R.W., Zhang, G.C., Zhang, H., Ye, T., 2011. Inhibition of PDGF, TGF-β, and Abl signaling and reduction of liver fibrosis by the small molecule Bcr-Abl tyrosine kinase antagonist Nilotinib. J. Hepatol. 55, 612–625.
Majumder, S., Piguet, A.C., Dufour, J.F., Chatterjee, S., 2013. Study of the cellular mechanism of Sunitinib mediated inactivation of activated hepatic stellate cells and its implications in angiogenesis. Eur. J. Pharmacol. 705, 86–95.
Miller, M.J., Foy, K.C., Kaumaya, P.T., 2013. Cancer immunotherapy: present status, future perspective, and a new paradigm of peptide immunotherapeutics. Discov. Med. 15, 166–176.
Mócsai, A., Kovács, L., Gergely, P., 2014. What is the future of targeted therapy in rheumatology: biologics or small molecules? BMC Med. 12, 43.
Papalia, G.A., Giannetti, A.M., Arora, N., Myszka, D.G., 2008. Thermodynamic characterization of pyrazole and azaindole derivatives binding to p38 mitogen-activated protein kinase using Biacore T100 technology and van't Hoff analysis. Anal. Biochem. 383, 255–264.
Patsenker, E., Popov, Y., Wiesner, M., Goodman, S.L., Schuppan, D., 2007. Pharmacological inhibition of the vitronectin receptor abrogates PDGF-BB-induced hepatic stellate cell migration and activation in vitro. J. Hepatol. 46, 878–887.

Prosser, C.C., Yen, R.D., Wu, J., 2006. Molecular therapy for hepatic injury and fibrosis: where are we? World J. Gastroenterol. 12, 509–515.
Reichenbach, V., Fernández-Varo, G., Casals, G., Oró, D., Ros, J., Melgar-Lesmes, P., Weiskirchen, R., Morales-Ruiz, M., Jiménez, W., 2012. Adenoviral dominant-negative soluble PDGFRβ improves hepatic collagen, systemic hemodynamics, and portal pressure in fibrotic rats. J. Hepatol. 57, 967–973.
Rodriguez, L.G., Wu, X., Guan, J.L., 2005. Wound-healing assay. Methods Mol. Biol. 294, 23–29.
Shim, A.H., Liu, H., Focia, P.J., Chen, X., Lin, P.C., He, X., 2010. Structures of a platelet-derived growth factor/propeptide complex and a platelet-derived growth factor/receptor complex. Proc. Natl. Acad. Sci. U. S. A. 107, 11307–11312.
Suzuki, N., Tsumoto, K., Hajicek, N., Daigo, K., Tokita, R., Minami, S., Kodama, T., Hamakubo, T., Kozasa, T., 2009. Activation of leukemia-associated RhoGEF by Galpha13 with significant conformational rearrangements in the interface. J. Biol. Chem. 284, 5000–5009.
Wang, X., Zhang, A., Gao, J., Chen, W., Wang, S., Wu, X., Shen, Y., Ke, Y., Hua, Z., Tan, R., et al., 2014. Trichomide A, a natural cyclodepsipeptide, exerts immunosuppressive activity against activated T lymphocytes by upregulating SHP2 activation to overcome contact dermatitis. J. Investig. Dermatol. 134, 2737–2746.
Wang, X., Wang, S., Hu, C., Chen, W., Shen, Y., Wu, X., Sun, Y., Xu, Q., 2015a. A new pharmacological effect of levornidazole: inhibition of NLRP3 inflammasome activation. Biochem. Pharmacol. 97, 178–188.
Wang, X., Zhou, Y., He, S., Ouyang, Z., Feng, L., Shen, Y., Wu, X., Sun, Y., Wu, X., Xu, Q., 2015b. Obaculactone exerts a novel ameliorating effect on contact dermatitis through regulating T lymphocyte. Int. Immunopharmacol. 28, 1–9.
Wear, M.A., Walkinshaw, M.D., 2006. Thermodynamics of the cyclophilin-A/cyclosporin-A interaction: a direct comparison of parameters determined by surface plasmon resonance using Biacore T100 and isothermal titration calorimetry. Anal. Biochem. 359, 285–287.
Westra, I.M., Oosterhuis, D., Groothuis, G.M., Olinga, P., 2014. Precision-cut liver slices as a model for the early onset of liver fibrosis to test antifibrotic drugs. Toxicol. Appl. Pharmacol. 274, 328–338.
Yoshida, S., Ikenaga, N., Liu, S.B., Peng, Z.W., Chung, J., Sverdlov, D.Y., Miyamoto, M., Kim, Y.O., Ogawa, S., Arch, R.H., et al., 2014. Extrahepatic platelet-derived growth factor-β, delivered by platelets, promotes activation of hepatic stellate cells and biliary fibrosis in mice. Gastroenterology 147, 1378–1392.
Zhang, A.H., Wang, X.Q., Han, W.B., Sun, Y., Guo, Y., Wu, Q., Ge, H.M., Song, Y.C., Ng, S.W., Xu, Q., et al., 2013. Discovery of a new class of immunosuppressants from Trichothecium roseum co-inspired by cross-kingdom similarity in innate immunity and pharmacophore motif. Chem. Asian. J. 8, 3101–3107.